XAFS Studies of Carboxypeptidase A: Detection of a Structural Alteration in the Zinc Coordination Sphere Coupled to the Catalytically Important Alkaline pK_a

Ke Zhang*

Biostructures Institute, University City Science Center, Philadelphia, Pennsylvania 19104

David S. Auld*

Center for Biochemical and Biophysical Sciences and Medicine and Department of Pathology, Harvard Medical School, Brigham and Women's Hospital, 250 Longwood Avenue, Boston, Massachusetts 02115

Received March 25, 1993; Revised Manuscript Received September 28, 1993®

ABSTRACT: X-ray absorption fine structure (XAFS) spectra of carboxypeptidase A (ZnCPD) show progressive spectral changes particularly in the near edge region when the pH is changed from neutral to alkaline values. Both least square fitting and radial distribution function (RDF) data analysis yield two distributions of atoms in the first coordination shell of ZnCPD at all pH values and at both 150 and 297 K. Direct comparison of the first and higher coordination shells of ZnCPD reveals structural differences between pH 7.0 and pH 9.9. At pH 7.0, the zinc ion has four ligand atoms (N or O) at an average distance of 2.024 ± 0.006 Å, and a smaller distribution of 1.3 atoms (N or O) at 2.54 ± 0.05 Å from the zinc ion (from the least square fitting analysis). At pH 9.9, the larger distribution contains four atoms at a 0.022 Å shorter distance (2.002 Å) from the zinc, while the smaller distribution contains 0.7 atom at 2.52 ± 0.06 Å. The smaller distribution can be attributed mainly to the contribution of the ϵ_2-oxygen of Glu 72 and to the atoms farther away for which the contribution cannot be fully separated from the first shell peak. The structural changes of ZnCPD at intermediate pHs are consistent with the changes observed at pH 7.0 and pH 9.9. The XAFS Debye–Waller factor shows an increased structural disorder for the four atom distribution at the alkaline pH. The higher shell comparison shows that the two histidine ligands His 69 and His 196 remain unchanged at the pHs examined. The plot of the normalized spectral changes at the absorption edge as a function of pH conforms to a theoretical pH-titration curve with a pK_a 9.49 at −4 °C. This value corresponds to that obtained by extrapolation of values of pK_{EH} by kinetic analysis of the carboxypeptidase-A catalyzed hydrolysis of tripeptides (Auld & Vallee (1971) *Biochemistry 10*, 2892). The pH-dependent shorter average metal–ligand distance and the increased first shell structural disorder is most easily explained by one of the other two metal ligands (the water molecule or the ϵ_1-oxygen of Glu 72) to the metal moving 0.09 ± 0.03 Å closer to the zinc ion at alkaline pH values. Such a situation could be due to either direct ionization of the metal bound water or an ionization-linked alteration in the coordination of Glu 72. As discussed herein, we favor assigning the alkaline pK_a in the kinetic profiles, pK_{EH}, to the ionization of the metal bound water molecule.

The study of the pH dependent properties of enzymes using a combination of physical and chemical techniques contributes to a better understanding of the mechanism of their catalytic function. In the zinc-containing bovine pancreatic carboxypeptidase A (ZnCPD[1]), enzyme catalysis of peptide and ester hydrolysis is strongly affected by pH. The pH dependence of the kinetic parameter k_{cat}/K_m is bell-shaped with two pK_a values of 6.0 and 9.0, independent of the peptide used (Auld & Vallee, 1970, 1971). Analysis of the individual k_{cat} and K_m profiles are supportive of a three protonation state model. According to this scheme, when the enzyme is in its EH_2 form below the acidic pK_{EH_2}, it can bind substrates but cannot hydrolyze them. The ionization of an enzyme group with a pK_{EH_2} value of 6.0 transforms the enzyme to its active form EH. Further ionization of the enzyme to the E form at pH 9.0 markedly reduces substrate binding and therefore the rate of catalysis.

Much attention has been devoted to elucidating the groups involved in determining the acid–base properties of the enzyme. It is likely that the acidic pK_{EH_2} reflects the ionization of COOH of Glu 270 or the metal ligated water molecule (Auld and Vallee, 1970). Ionization of either can promote the formation of a hydrogen bond between the Glu 270 carboxyl group and the water ligand of the zinc, ultimately stabilizing the active site structure (Auld & Vallee, 1987; Christianson & Lipscomb, 1989). This is consistent with the X-ray crystallographic results (Lipscomb, 1974) that the interatomic distance from active site zinc to the carboxylate of Glu 270 is about 4.5 Å, a distance consistent with a hydrogen bond between the metal bound water molecule and Glu 270.

The assignment of the group responsible for the alkaline pK_{EH} has long been in dispute and conjecture (Vallee et al., 1963; Kaiser & Kaiser, 1972; Lipscomb, 1974; Spratt et al., 1983; Vallee et al., 1983; Auld et al., 1986; Mock & Tsay, 1988; Auld et al., 1992). The accumulated evidence supports the assignment of the alkaline pK_a to either Tyr 248, the zinc bound water molecule, or a histidyl ligand. Examination of pH-activity profile for the nitro- and aminoenzyme, NO_2-

® Abstract published in *Advance ACS Abstracts*, November 15, 1993.

[1] Abbreviations: ZnCPD, carboxypeptidase A; Im, imidazole; Ac, acetate; FaFF, *N*-(2-furylacryloyl)-L-phenylalanyl-L-phenylalanine; Tris, tris(hydroxymethyl)aminomethane; Mops, 3-(*N*-morpholino)propanesulfonic acid; Mes, 2-(*N*-morpholino)ethanesulfonic acid; Hepes, *N*-2-(hydroxyethyl)piperazine-*N*′-2-ethanesulfonic acid; Ches, 2-[*N*-cyclohexylamino)ethanesulfonic acid; Caps, 3-*N*-(cyclohexylamino)-propanesulfonic acid.

0006-2960/93/0432-13844$04.00/0

Tyr-248 and NH_2-Tyr-248, led to the suggestion that the ionization of Tyr 248 leads to the same effect on activity as does the ionization of the group responsible for the alkaline pK_a of the native enzyme (Auld et al., 1986). ^1H NMR studies of the pH dependence of inhibitor binding to the cobalt enzyme (Auld et al., 1992) has put in doubt the assignment of His 69 or 196 to this ionization (Mock & Tsay, 1988). A role for the ionization state of Tyr 248 is in accord with the notion that this amino acid has some role in peptide binding as indicated by site directed mutagenesis studies and the kinetics of the nitro-Tyr 248 enzyme (Gardell et al., 1985; Hilvert et al., 1986; Auld et al., 1986).

Electronic absorption and ^1H NMR studies of the cobalt enzyme and its inhibitor complexes as a function of pH provide evidence for pK_{EH} being related to a group close to or within the metal coordination sphere (Latt & Vallee, 1971; Auld et al., 1992). Furthermore, it has been shown by the kinetic measurements that (Auld & Vallee, 1970) the reduced enzyme activity toward peptide hydrolysis at the alkaline pK_a is due to reduced substrate binding. This reduction in binding would be expected if the water ligand is ionized at alkaline pH, since the displacement of metal bound hydroxide is more difficult than a water ligand.

X-ray absorption fine structure (XAFS) is a quantitative experimental technique to probe the local environment around metal ions (Stern & Heald, 1983). Previously, we have used XAFS to compare the local structure of the metal ion in Zn- and CoCPD, and found that their solution metal ion coordination sphere differs from that in their crystalline state counterparts particularly in the position of the fifth ligand (Zhang et al., 1992). The first coordination shell of the zinc ion was resolved into two distribution of atoms with the error of the average distance determination of the major distribution to be about 0.01 Å. In addition, XAFS studies can provide unique information about the displacement of atomic pairs about their mean distance, through the XAFS Debye–Waller factor. Thus, fine structural details, such as slight interatomic distance, and disorder changes at the active site that originate from the protonation of a metal ligand, may be detectable by XAFS experiments. We have therefore examined the XAFS spectra of carboxypeptidase A from the neutral to alkaline pH region with the goal of detecting any pH dependent structural changes in the zinc coordination sphere.

MATERIALS AND METHODS

Enzyme Preparation. Carboxypeptidase A from bovine pancreas prepared according to the method of Cox et al. (1964) was obtained from Sigma Chemical Co., St. Louis, MO (C-0261, lot no. 10H8040).

The crystalline suspension was collected by centrifugation at 8000 rpm at 4 °C using a Sorvall HB-5B, and the pellet was washed with 50 mM Hepes, pH 7.5 buffer. After centrifugation the pellet was dissolved in 2 M NaCl, 50 mM Tris, pH 7.55 buffer to an estimated concentration of about 100 mg/mL of enzyme. This solution was centrifuged at 12 500 rpm for 5 h to remove a small amount of yellow-brown particulate matter. The slightly yellow enzyme solution is then purified by affinity chromatography at 4 °C (Bazzone et al., 1979). Approximately 90% of the purified enzyme is collected in two 11-mL fractions from the column. The purified enzyme was recrystallized by dialysis against 10 mM Tris, pH 7.5 at 4 °C.

Preparation of XAFS Samples. The buffers used to control pH were usually at pH values near their pK_a at 25 °C: Mes (pK_a, 6.10), Mops (pK_a, 7.10), Hepes (pK_a, 7.5), Ches (pK_a, 9.25), and Caps (pK_a, 10.3). Caps was recrystallized from ethanol/H_2O before using. All other buffers (Research Organics) were used directly. The buffer concentration was usually 100 mM. The 1 M NaCl concentration was to insure the solubility of the enzyme, whose concentration was in the range 1.7–2.4 mM. The pH of the solution was measured at 25 and 0 °C. The pH meter was standardized with pH 7 and 4 buffers at the indicated temperatures. The value of the pH 10 standard was within 0.05 unit of its expected value. The 1 M NaCl solutions used in these studies solidify in the temperature range −3 to −5 °C as expected (Lange, 1956). The metal complex, $Zn(Im)_2(Ac)_2$, was prepared (Horrocks et al., 1980) to approximate the backscattering amplitude as well as central and backscattering phase shifts for the first coordination sphere of zinc ion in ZnCPD.

XAFS Measurement. XAFS experiments were conducted on beamline X9-A at the National Synchrotron Light Source of Brookhaven National Lab. The Biostructures Participating Research Team beamline is equipped with a double crystal, constant exit height monochromator, and a Ni coated Al harmonic rejection mirror. All of the data were collected using the monochromator with Si(220) crystals and a fixed vertical opening of about 0.8 mm for beam entry in the experimental hutch to insure high and precise energy resolution. A helium close cycle Displex refrigerator was used to control the sample temperature with an accuracy of better than 1 deg Kelvin. Pure copper sample holders were used for the low-temperature measurement, while plastic sample holders were used at room temperature to avoid interaction of copper with the protein over the several hour period of data collection. Zn K_a fluorescence from the sample after absorption of the X-ray photons was collected using a 13-element Ge detector (Canbarra GL0110). The dead-time loss of the detector system was calibrated on-line for a wide range of incident count rates on each sample, which was corrected by the approximation of the paralyzable model (Zhang et al., 1993). The incident count rate of the detector was maintained at about 80 000 per channel during the experiments, which is much less than the saturation value of the detector.

ZnCPD samples of pH 7.0, 7.9, 8.47, 9.04, 9.2, and 9.9 were measured at 150 K. Near edge spectra alone were obtained for samples of pH 7.9 and pH 10.8 at room temperature. The pH values of all the samples were measured with a microelectrode (Aldrich Z1134-5) immediately before and after the XAFS measurement at room temperature. A maximum change of 0.1 pH unit was observed. A zinc complex, $Zn(Im)_2(Ac)_2$, was also measured by applying its fine crystalline powder on a piece of Scotch tape. No protein precipitation nor progressive spectral changes were observed during the measurements. A series of scans were collected for a total of several million effective signal counts on each sample.

Since the pH values of the ZnCPD samples were monitored at 25 and 0 °C, while the XAFS measurements were performed mainly at 150 K, the temperature dependence of the pH value of the buffer solution had to be taken into account. The pH values were extrapolated to −4 °C, the freezing point of the buffer solution (Lange, 1956). These pH values and the buffer solutions used are listed in Table I. We further assume that the pH value remains the same once the buffer solution is frozen. Thus, the proportion of the acid and basic forms of any protein ionizing group at 150 K is the same as that at −4 °C. Unless specifically mentioned, the pH values used in the

Table I: Sample pH, Buffer Solution, and X-ray Absorption Edge Feature

pH at 25 °C	buffer	pH at −4 °C	spectral difference[a]
7.00	Mops	7.2	0.134
8.00	Hepes	8.4	0.115
8.50	Hepes	8.9	0.084
9.04	Hepes/Caps	9.7	0.046
9.18	Ches/Caps	10.0	0.002
9.9	Hepes/Caps	10.6	−0.010

[a] These are the intensity difference relative to the edge step for the peaks located at 9.659 and 9.664 KeV of the X-ray absorption spectra. The error of the pH value is 0.1 unit.

following discussions are the ones measured at room temperature.

Data Reduction and Analysis. The XAFS formula for the single scattering and the K-edge absorption is given by (Stern, 1974)

$$\chi(k) = \sum_j \frac{N_j B_j(k)}{kR_j^2} \sin [2kR_j + \delta_j(k)] \exp(-2R_j/\lambda) \exp(-2k^2\sigma_j^2) \quad (1)$$

The sum is over atomic coordination shell j with coordination number N_j and at distance R_j from the absorbing atom. The B_j and δ_j are the functions describing the back-scattering amplitude and central and back-scattering phase shift; σ^2 is the mean-square variation of the atomic distance about its mean distance R_j; λ and k are the photoelectron mean free path and wave number, respectively. The phenomenological mean free path term, $\exp(-2R_j/\lambda)$, accounts for photoelectron finite lifetime effects.

The XAFS data analysis procedure used previously (Zhang et al., 1992) was closely followed. The atomic absorption background was subtracted using a three-region cubic spline fit. Pseudoradial distribution of atoms was obtained by a Fourier transform with k^2 weighting and isolated by a back-transform with a desired window function. Least-squares fitting and the radial distribution function (RDF) method (Bouldin, 1984; Crozier et al., 1988; Stern et al., 1992) were used to obtain structural information for a single coordination shell using empirical model compounds.[2] As stated, previously, the combined use of the least-squares fitting and RDF methods in our XAFS data analysis is to provide a less biased structural determination as well as precise structural parameters and to perform error analysis. A previously proposed (Zhang et al., 1988) fitting criterion has been used to determine whether a fitting model will be accepted or rejected.

The relative mean-square radial displacement of atoms σ^2, contained in the XAFS Debye–Waller factor term, can be examined experimentally. The XAFS Debye–Waller factor consists of mathematical terms reflecting structural and thermal disorder, that can be separated by temperature dependent experiments. At sufficiently low temperatures, where the thermal disorder can be neglected, the σ^2 term is a combination of structural disorder and the disorder due to quantum zero point motion. For similar systems, the zero point motions are about the same. For a coordination shell of atoms with a single Gaussian distribution, the XAFS Debye–Waller factor is usually examined by the ratio method (Bunker, 1983). In the first shell of ZnCPD, where two atom distributions are present (Zhang et al., 1992), the ratio method is not applicable for determining the Debye–Waller factor of a particularly distribution. Fortunately, the Debye–Waller factors can be examined by the width of individual distributions in the RDF, so long as the two atom distributions are separable. The Debye–Waller factors so obtained are believed to be more reliable than the fitting method, since the coordination number and its disorder are less correlated in the RDF method.

It is a general assumption that the mean free path term is cancelled when comparing an XAFS spectrum of a sample with a similar model compound. Generally speaking, this approximation is a good one, that has been used previously (Zhang et al., 1992). However, the mean free path term is dependent on the interatomic distance R. This term will not be cancelled out completely when the interatomic distance of the sample is substantially different from that of the model. For example, modeling of a distribution of atoms at 2.50 Å with a distribution of atoms at 2.00 Å will result in a reduced coordination number. We calculated λ for the Zn ion coordinated with two oxygens and two nitrogens using the FEFF program (Mustre de Leon et al., 1991). From k = 2.5–10 Å^{-1}, λ changes from 5.3 to 15 Å. To simplify the correction, λ will be approximated by an average value, equal to 7.5 Å. With this simplification, the correction factor, $\exp(2(R_2-R_1)/I)$, is a constant acting upon the XAFS amplitude, where R_1 and R_2 are the bond lengths for the reference compound and the enzyme, respectively.

Assessment of Radiation Damage. No time dependent changes in the XAFS spectra are observed during the experiment. The thawed samples after X-ray irradiation contain no precipitated protein. No effects on enzymatic activity nor amino acid composition have been noted (Zhang et al., 1992).

RESULTS

The XAFS absorption near edge spectra for ZnCPD at pH 7.0, 9.04, and 9.9 at 150 K are directly compared in Figure 1A. The relative height of the two peaks located at energies 9.659 and 9.664 KeV (Figure 1A) on the edge changes substantially from pH 7.0 to pH 9.9. Since the near edge region is sensitive to the coordination geometry of the zinc ion, the differences suggest that structural changes occur at the active site as a function of the change in pH. The difference of the two peaks relative to the edge step for the enzyme at different pH values changes systematically from 0.13 at pH 7.0 to −0.01 at pH 9.9, demonstrating its pH dependent nature (Table I). The near edge spectra of ZnCPD at room temperature are shown in Figure 1B for pH 7.9 and 10.8. The features of the spectral differences observed at the low temperature are retained at room temperature. The features are broadened when compared to those obtained at the low temperature, as expected due to the increased thermal disorder at the higher temperature. The XAFS $\chi(k)$ function at pH 7.0, 9.04, and 9.9 are shown in Figure 2. The χ data are Fourier transformed from 1 to 12.5 Å^{-1} in k-space (Figure 3). Again, both the XAFS raw data and their Fourier transforms show a progressive change with the increase of pH. Back Fourier transforms are performed for the first coordination shell located between 0.7 and 2.3 Å, and for the higher coordination shell located between 2.8 and 4.1 Å in R-space. The spectrum at pH 8.47 as well as that for $Zn(Im)_2(Ac)_2$ were treated in the same fashion (data not shown).

The RDFs of the first coordination shell, calculated for pH 7.0 and 9.9, are shown in Figure 4. The RDFs are constructed

[2] Model compounds are structurally characterized metal complexes that are used as standards of reference.

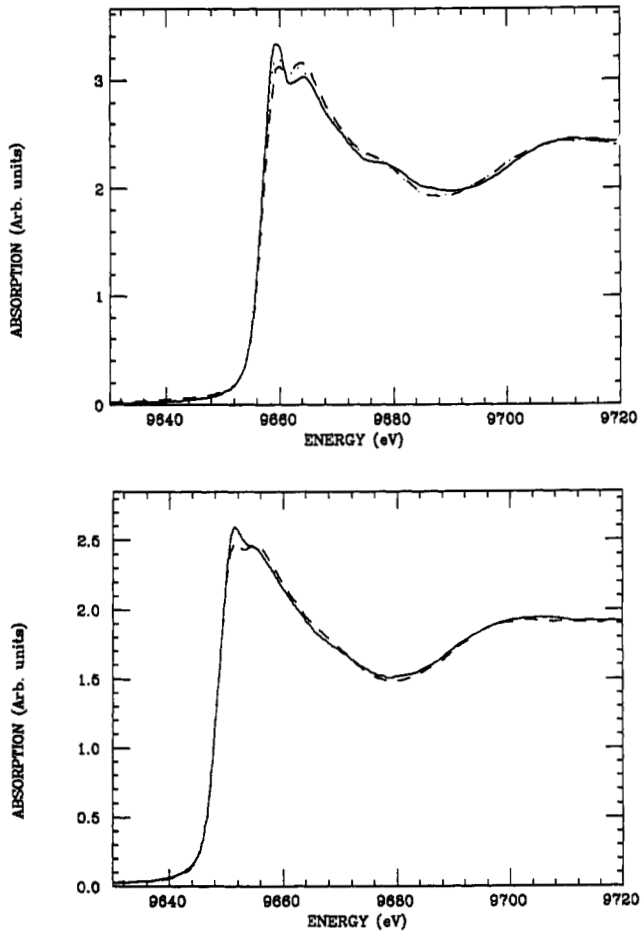

FIGURE 1: (A) Zn K-edge X-ray absorption near-edge spectra vs the X-ray energy for ZnCPD at pH 7.0 (solid) pH 9.04 (dot) and pH 9.9 (dash). The spectra are measured at 150 K. The double peak feature located at 9.659 and 9.664 KeV of the absorption edge is indicated. (B) The near edge spectra of ZnCPD at pH 7.9 (solid) and pH 10.8 (dash) measured at room temperature.

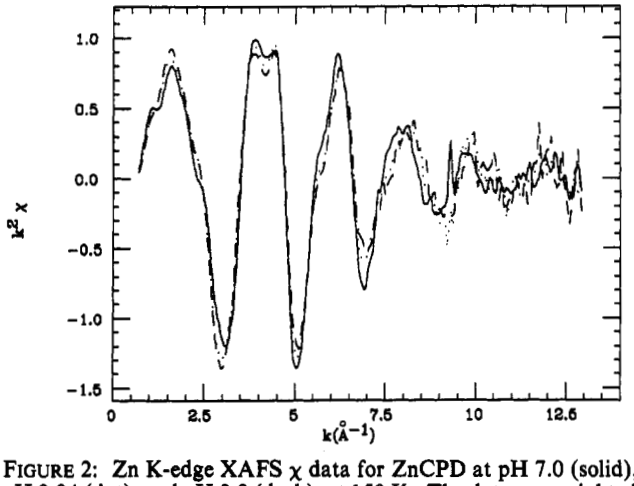

FIGURE 2: Zn K-edge XAFS χ data for ZnCPD at pH 7.0 (solid), pH 9.04 (dot), and pH 9.9 (dash), at 150 K. The data are weighted with a k^2 factor.

by cancellation of the central and back-scattering phase shifts and the back-scattering amplitude by taking the amplitude ratio and phase difference between the enzyme and $Zn(Im)_2(Ac)_2$. The amplitude ratio and the phase difference are extrapolated to $k = 0$ by a cumulant expansion, followed by an inverse sine transform to obtain the RDFs. The photoelectron lifetime effects are corrected with a constant mean free path $\lambda = 7.5$ Å. As previously reported for the pH 7.0 form of ZnCPD (Zhang et al., 1992), the RDFs for all the

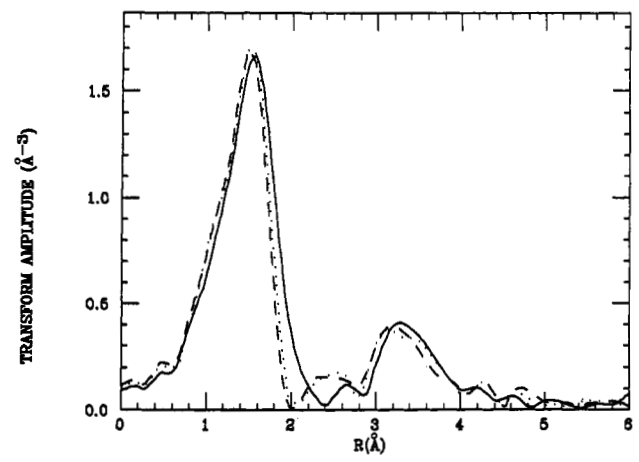

FIGURE 3: Fourier transforms of the XAFS χ (k) data of ZnCPD, shown in Figure 2, at pH 7.0 (solid), pH 9.02 (dot), and pH 9.9 (dash). The $k^2\chi$ Fourier transform is performed from 1 to 12.5 Å^{-1} in k-space.

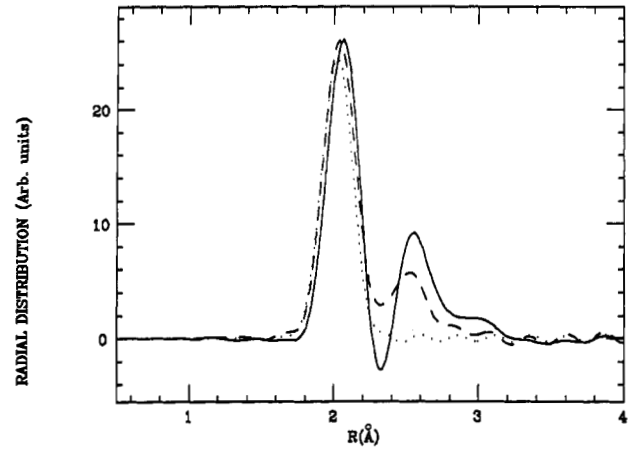

FIGURE 4: The RDFs of ZnCPD measured at pH 7.0 (solid) and pH 9.9 (dash), compared with the RDF calculated for the reference complex $Zn(Im)_2(Ac)_2$ (dot), which is used to obtain the RDFs. The distributions are broadened by a Gaussian factor of $\sigma_c^2 = 0.01$ Å^2 to reduce the truncation effects.

pH values consist of two distributions. The larger distribution of pH 7.0 contains about 4.2 atoms (nitrogen or oxygen) at 2.025 ± 0.006 Å, and the smaller distribution contains 1.3 atoms (nitrogen or oxygen) at 2.55 ± 0.04 Å. Differences are found by comparing the RDF at pH 7.0 and pH 9.9. The average distance of the larger distribution (containing about 4.2 nitrogens or oxygens) from the zinc ion is shortened by about 0.023 Å to 2.002 ± 0.006 Å at pH 9.9. Furthermore, the smaller distribution was substantially reduced to about 0.7 atom (nitrogen or oxygen) located at 2.49 ± 0.06 Å. The locations and the amplitudes of the RDFs at intermediate pH values are consistent with those obtained for the pH 7.0 and pH 9.9 forms of the enzyme.

The least-squares fitting results for the first shell of ZnCPD are summarized in Table II along with a measure of the quality, Q, of the fit. The fitting is performed between 2.0 and 10.0 Å^{-1} in k space to insure enough degrees of freedom and good signal-to-noise ratio. Taking the back-transform window used to be 1.6 Å, this data range gives about 8 deg of freedom (Lee et al., 1981). The quality of both single and double distance fitting models is evaluated according to the expression given previously (Zhang et al., 1988). A fit can be accepted when the quality Q is close or less than one and rejected if much greater than one. The results are corrected for the photoelectron lifetimes effects as described in Materials and

Table II: First Shell Fitting Results of ZnCPD at 150 K[a]

	2-distance model				1-distance model			
samples	N	R (Å)	σ^2 (Å^2)	Q	N	R (Å)	σ^2 (Å^2)	Q
ZnCPD pH 7.0	4	2.024(6)	–0.0006	1.0	3.7(14)	2.03(2)	0.0005	16
	1.3(4)	2.54(5)	–0.0012					
ZnCPD pH 8.47	4	2.015(6)	–0.0002	0.4				
	1.0(4)	2.52(5)	0.0007					
ZnCPD pH 9.04	4	2.009(6)	–0.0003	0.5				
	0.8(5)	2.52(5)	–0.0014					
ZnCPD pH 9.9	4	2.002(6)	0.0007	0.3	3.9(6)	2.003(8)	0.0003	1.2
	0.7(5)	2.52(6)	0.0020					

[a] The value in the parentheses is the ± error in the last digit.

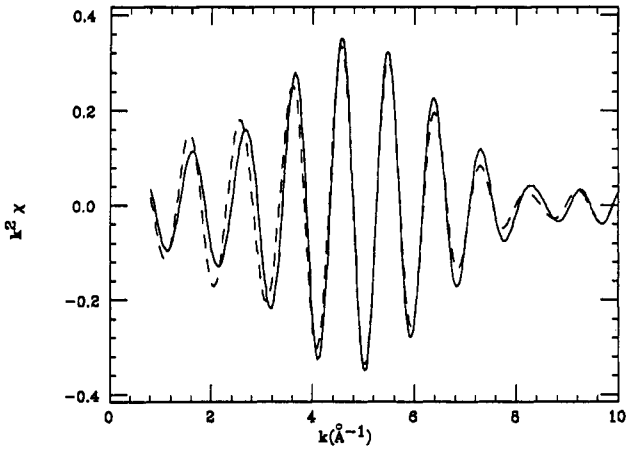

FIGURE 5: XAFS χ data of the higher shell peak isolated between 2.8 and 4.1 Å in the Fourier transform of Figure 3 for ZnCPD at pH 7.0 (solid), pH 9.04 (dot), and pH 9.9 (dash). The signal is due to γ-carbon and δ_1-nitrogen of the histidine ligands.

Methods. The single distance fit of ZnCPD at pH 7.0 results in a Q value of 16, clearly cause for rejection of this model (Table II). On the other hand, a good fit is obtained using the two distance model (Q = 1.0). For the pH 9.9 data, the two distance model still gives the better fit to the data (Q = 0.3). However, the single distance model gives an acceptable result (Q = 1.2). Consistent with the RDF results, four atoms (nitrogen and oxygen) are found at 2.024 ± 0.006 Å, and 1.3 ± 0.4 atoms are found at 2.54 ± 0.045 Å in the first shell of ZnCPD at pH 7.0. At pH 9.9, the four atoms were found at an average distance of 2.002 ± 0.006 Å, and the smaller distribution of 0.7 ± 0.5 atom is found at 2.52 ± 0.06 Å. The reason for an acceptable single distance model at pH 9.9 is due to the decreased contribution of the smaller distribution. The structural changes determined by the fitting procedure for the intermediate pHs are consistent with the changes observed from pH 7.0 to 9.9. For example, the change of the average distance for the four atom distributions is 0.008 Å between pH 7.0 and 8.47, and 0.014 Å between pH 7.0 and pH 9.04, compared to the change of 0.022 Å between pH 7 and pH 9.9. The coordination number of the small distribution of atoms progressively changes from 1.3 at pH 7.0 to 1.0 at pH 8.47 to 0.8 at pH 9.04.

A qualitative comparison can be made for the higher coordination shell contribution located between 2.8 and 4.1 Å of the Fourier transform. The isolated χ functions of the higher shell contribution at pHs 7.0, 9.0, and 9.9 are shown in Figure 5. The signal is contributed mainly by γ-carbon and δ_2-nitrogen of the coordinated histidine ligands, which is largely enhanced by the focusing effect (Bunker et al., 1982). However, many multiple-scattering paths with path length around 8 Å will contribute to this peak, including most of the double scattering paths between the atoms located within 3 Å from the zinc ion. However, multiple-scattering contributions will diminish with the increase of electron wave number k (to about 4 Å^{-1}) as determined for $GeCl_4$ (Bouldin et al., 1988). Without going into a detailed multiple-scattering calculation, some insights can be inferred from the spectra. The small differences at higher k-region (4–8 Å^{-1}) between pH 9.9 and pH 7.0 indicate that little structural change occurs for the histidines that bind the zinc. Analyzed by the ratio method (Bunker, 1983), the XAFS phase difference in this region shows a 0.00 ± 0.04 Å distance change for the γ-carbon and the δ_2-nitrogen of the coordinated histidine ligands. Phase differences, close to the absorption edge ($k \leq 4$ Å^{-1}), are found between the alkaline pH data and the neutral pH data. This suggests that structural changes occur for atoms within 3 Å of the metal from neutral pH to alkaline pH values, which may be largely due to binding angle changes. The combined observations suggest the inner coordination sphere changes are likely due to changes in the ligation properties of Glu 72 and/or the bound water molecule.

Table III: Relative XAFS Debye–Waller Factor for ZnCPD at Different pHs[a]

sample ZnCPD/$Zn(Im)_2(Ac)_2$			
pH	T (K)	ref T (K)	σ^2 (Å^2 × 10^{-3})
7.0	150	130	0.7(5)
9.9	150	130	2.0(5)

[a] The values in the parentheses are the ± errors in the last digit.

The width of the larger distribution of the RDF of the enzyme relative to that of $Zn(Im)_2(Ac)_2$ are determined for the 150 K data. This gives an assessment of the relative structural disorder for the four atoms. The σ^2 changes are listed in Table III for ZnCPD at pH 7.0 and 9.9. The disorder of the four atoms at pH 7.0 is found to be slightly larger than that of $Zn(Im)_2(Ac)_2$. This can be attributed to the increased structural disorder and the zero point motion (Sevillano et al., 1979) in the protein. Strikingly, a larger σ^2 difference, about 0.002 Å^2, is found for the protein at pH 9.9. Assuming the disorder caused by the zero point motion at both pHs is about the same, this gives an increased structural disorder of 0.0013 Å at pH 9.9 compared with that at pH 7.0. The increase of the structural disorder is also observed at intermediate pH values, although to a lesser extent.

DISCUSSION

XAFS, a direct structural technique suitable for both solution and condensed states, can provide detailed information on the metal binding sites for biological systems. Subtle structural changes, corresponding to 0.03 Å for individual first shell distances, can be detected by XAFS (Cramer, 1988). This translates to an accuracy of about 0.01 Å for the first shell average distance. Since part of the distance uncertainty

is due to the transferability of phase shift, the accuracy in comparing the average distance changes in the same protein is expected to be better than 0.01 Å. The fine structural details provided by XAFS in the solution state can aid therefore in elucidating the mechanistic consequences of structural changes in the metal coordination sphere of metalloenzymes. Thus, a comparative XAFS study from neutral pH to alkaline pH values can probe detailed structural changes at the active site of ZnCPD as a function of the ionization states that affect activity.

XAFS least square fitting data analysis of the first coordination shell of the enzyme at pH 7.0 reveals two distributions of atoms with four atoms (nitrogen and oxygen) and 1.3 atoms (nitrogen or oxygen) each located at 2.024 Å and 2.54 Å from the zinc ion, respectively. Progressive spectral changes of ZnCPD are observed from pH 7.0 to pH 9.9. Both the RFD and least-squares fitting analysis on the first shell of ZnCPD at pH 9.9 determine two distributions of atoms with four atoms and less than one atom, respectively. The four atom distribution is found at a 0.022 Å shorter distance from the metal ion than that at pH 7.0. The comparisons of the higher shell χ data and the near edge spectra between pH 9.9 and 7.0 indicate that the two histidine ligands remain unchanged (within the experimental error of 0.04 Å) and suggest that substantial rearrangement involving other first shell ligands occurs (Figure 5). XAFS Debye–Waller factor yields further information about the structural changes. The relative mean squares displacement of the four atom distribution at 150 K and pH 9.9 is found to be about 0.0013 Å^2 larger than that at pH 7.0 (Table III). The results of the intermediate pH values distribute consistently within the range defined by the two pH extremes of 7.0 and 9.9.

The fractional coordination number for the smaller first shell distribution changes from 1.3 to 0.7 as a function of pH. It can be argued that a fractional coordination is possible since proteins can exist in different conformations, particularly when examined over a wide pH range. However, this can also be attributed to coordination number errors through both experimental and data analysis procedures. This is particularly acute when examining a distribution of atoms in the outer coordination shell. In this case the coordination number error can be introduced by data analysis from two major sources. First, as described previously, the uncertainty of the lifetime of photoelectron can bring in a large error in the coordination number determination. The lifetime effect is represented by a mean-free path term in the XAFS formulation (Stern & Heald, 1983). Using $Zn(Im)_2(Ac)_2$, which has two nitrogens and two oxygens in its first coordination shell at an average distance of 1.986 Å, this term may be canceled out for the four atom distribution in the first shell of ZnCPD. However, this mean-free-path term will not be canceled out for a distribution of atoms farther away. The effect of the finite lifetime of the photoelectron is to underestimate the coordination number for the atoms farther away than those of simpler zinc complex species. A simplified lifetime correction, in which λ was approximated as a constant, is implemented in the data analysis.

The second source of the coordination number error is due to the interference between different coordination shells in the Fourier transform. Previously, the four atom distribution has been assigned to the two δ_1-nitrogens of His 96 and 196, the ϵ_1-oxygen of Glu 72, and the oxygen of the coordinated water, and the smaller distribution to the ϵ_2-oxygen of Glu 72 (Zhang et al., 1992). According to this assignment, the carbon atom of COO^- of Glu 72, and the α- and β-carbons of His 69 and 196 are located between about 2.7 and 3.1 Å from the zinc ion. Therefore, a clean separation of the signals of these five atoms using a back Fourier transform is essentially impossible. The interference among atoms at different distances, which are not fully separated in the back transform, can result in variation in coordination number.

Thus the error introduced by the uncertainty of the photoelectron lifetime and the contribution of other atoms outside of the first coordination shell preclude a precise quantitative conclusion as to why the coordination number of the fifth ligand changes with pH. It can be speculated that the apparent decreased intensity of the fifth ligand is either due to increased disorder and/or a decrease in the coordination number by a change in the protein conformation as a result of the average distance change for the other four ligands. Thus a shortened zinc–ligand bond distance of the four inner sphere ligands likely weakens the bond between zinc and the fifth ligand. This would result in increased disorder or/and reduced coordination number.

The effect of pH on the Debye–Waller factor, higher shell structure, and the interatomic distance can aid in deciphering the origin of the structural changes in the zinc coordination site over the neutral to alkaline pH range (Table II and III, Figures 4 and 5). X-ray diffraction studies show that the four ligands of the zinc ion in $Zn(Ac)_2(Im)_2$ are distributed evenly at an average distance of 1.986 Å (Horrock et al., 1980) with a small structural mean-square displacement of 0.0003 Å^2. The small σ^2 increase from $Zn(Ac)_2(Im)_2$ to ZnCPD at pH 7.0 and 150 K demonstrates that the four atoms in ZnCPD are distributed somewhat evenly (on average, within 0.03 Å from their mean distance). The increase of the Debye–Waller factor for ZnCPD at pH 9.9 indicates an increased disorder in the arrangement of the ligands about the zinc. A marked change of interatomic distance for one or two ligands will introduce such an increased structural disorder. In our case, the 0.022 ± 0.006 Å average distance change for the four atoms is equivalent to a 0.09 ± 0.03 Å distance change for a single ligand, provided that the other three ligands remain at the same distance (within the experimental error of 0.01 Å). This will result in an increase of the XAFS Debye–Waller factor of 0.0012 Å^2 for the four atom distribution, which is consistent with the increase of the structural disorder found at pH 9.9.

The decrease of interatomic distance for a single ligand could be due to any of the zinc ligands, i.e., the two δ_1-nitrogens of His 69 and 196, the ϵ_1-oxygen of Glu 72 or the water molecule. The higher shell analysis shows that the two histidines remain at the same distance (within the experimental error of 0.04 Å) from the metal ion at pH values of 7.0, 9.0, and 9.9. Thus the decrease of interatomic distances of 0.09 Å from one of the δ_1-nitrogens to the Zn ion can be ruled out. ^{1}H NMR spectroscopy of the isotropically shifted signals in cobalt carboxypeptidase A, ascribed to the NH proton of His-69 and to the C-4 protons of His-69 and His-196, also do not change markedly over the neutral to alkaline pH range, again suggestive of no major changes in the His ligand conformation with pH (Auld et al., 1992).

Since the ligand Glu 72 would be deprotonated in its ligated state it cannot be directly responsible for the ionization associated with the change in ligand distance. In order for it to be responsible it would have to be correlated to a change in protein conformation associated with ionization of another amino acid residue, e.g., Tyr 248 (Auld et al., 1992). A rotation of Glu 72 that brings its ϵ_1-oxygen closer to the zinc might be accompanied by a movement in its ϵ_2-oxygen to a position

further away yielding both an increase in the Debye–Waller factor and a decrease in the amplitude of the 2.5 Å contribution as is observed. However, X-ray diffraction studies have not indicated any such associated interactions for Glu 72 (Rees et al., 1983; Shoham et al., 1984). Studies at pH values of 7.5, 8.5, 9.0, and 9.5 indicate zinc remains ligated to His 69, His 196, both oxygens of Glu 72, and a water molecule in the crystalline state (Shoham et al., 1984). The authors were reluctant to assign any chemical significance to slight structural changes in any ligand since the changes were all within the at least ±0.2 Å standard deviation in the atomic positions of the X-ray crystallographic study. Very little movement of the polypeptide backbone was seen as a function of pH. The two side chains that exhibited the highest deviation at high pH values, Ser 159 and Thr 293, are located more than 25 Å from the binding site on the surface of the molecule. In general it was noted that deviating side chains of residues were on the surface, 15 Å or more from the active site, and their movement did not appear to be correlated with the alkaline pK_a value (Shoham et al., 1984).

Water is the one ligand which of course could ionize and whose distance from zinc might be expected to decrease upon forming the anion, hydroxide. This ionization likely also would interfere with the Glu 270 and zinc bound water hydrogen bonding interaction. In addition, the decrease in Zn–OH distance would strengthen this bond and could lead to a slight weakening of the zinc–Glu 72 interaction with an associated increase in the distance of the Glu 72 oxygens from the zinc. Such a result would also contribute to the observed larger Debye–Waller factor and decrease in the amplitude associated with the fifth ligand.

Enzymatic activity has long been known to depend on a pK_a of 9.0 at 25 °C (Auld & Vallee, 1970, 1971). Ionization of a group (EH $\rightleftharpoons$ E) results in loss of peptide binding. Direct examination of the interaction of substrates with the cobalt enzymes at subzero conditions suggests the peptide perturbs the inner sphere coordination of the cobalt ion at pH 7.5 possibly through interaction with its amide carbonyl group (Auld et al., 1984). The formation of the ES complex could therefore displace or rearrange the water to promote its participation through general acid/base catalysis by Glu 270. If the water is converted to hydroxide ion substrate binding should be impeded as is observed (Auld & Vallee, 1970a,b). The results of recent ^{1}H NMR studies of the pH-dependent properties of inhibitor binding to cobalt carboxypeptidase A are also consistent with the assignment of pK_{EH} to that of the metal bound water (Auld et al., 1992).

Extrapolation of the kinetic data obtained for the temperature dependence of pK_{EH} (Auld & Vallee, 1971) to –4 °C, the freezing point of these 1 M NaCl solutions (Lange, 1956) yields a value of 9.49 (Figure 6). To examine how closely the XAFS spectral changes are related to this catalytically important protonation state of the enzyme, the spectral changes at the near edge region as a function of pH are fitted to a theoretical titration curve. Assuming the pH values remain the same in its frozen states, the comparison can be made at the freezing point of the buffer solution used. The solid line plotted in Figure 7 is a theoretical titration curve for the conversion of the active EH form of the enzyme to its inactive counterpart, E, occurring with a pK_a of 9.49 (at –4 °C). The changes of the normalized differences in Table I vs pH closely resembles the theoretical titration curve, indicating that the conversion of EH into E is responsible for the observed structural change in the metal coordination sphere.

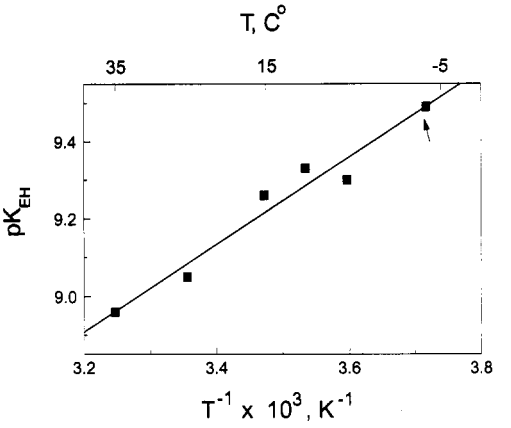

FIGURE 6: The temperature dependence of pK_{EH} as determined for the carboxypeptidase A catalyzed hydrolysis of tripeptides (Auld & Vallee, 1971). The extrapolated value of pK_{EH} for –4 °C used for the XAFS titration curve in Figure 7 is indicated by the arrow.

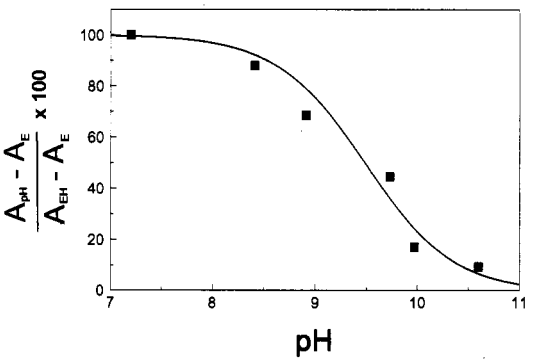

FIGURE 7: Plot of the normalized spectral difference between the peaks located at 9.659 and 9.664 KeV of the absorption edge (Figure 1A), compared with the theoretical titration curve with a pK_a equal to 9.49. The spectral differences were normalized to the edge step and fitted using the amplitude A_{EH} at pH 7.4 at –4 °C as that for the active enzyme species, EH, and the value of the amplitude at pH 10.6 as being 90% converted to E. This allows calculation of the amplitude difference between EH and E. The theoretical curve was generated using the pH values for the buffers extrapolated to –4 °C.

To summarize, the XAFS study clearly demonstrates progressive structural changes in the zinc coordination sphere of ZnCPD from neutral pH to alkaline pH values. The plot of the normalized spectral changes in the near edge region as a function of pH conforms to a theoretical titration curve with a pK_a equivalent to that found for the enzyme in pH-activity profiles (Figures 6 and 7). The structural changes can be attributed to the ionization of the water coordinated to the zinc ion. This ionization would be expected to strengthen the Zn–OH bond and thus prevent substrate and inhibitor binding that requires displacement of the zinc bound water. Thus, it is likely that the ionization of the ligated water molecule in ZnCPD is responsible for the alkaline pK of the enzyme and leads to the diminished enzymatic activity at high pH values.

ACKNOWLEDGMENT

The research reported here was supported by NIH Grants RR-01633 and GM-47534. We appreciate the support of the staff of the NBPRT beamline X9-A and National Synchrotron Light Source.

REFERENCES

Auld, D. S. (1988) *Methods Enzymol. 158*, 71.
Auld, D. S., & Vallee, B. L. (1970) *Biochemistry 9*, 4352.

Auld, D. S., & Vallee, B. L. (1971) *Biochemistry 10*, 2892.
Auld, D. S., Goldes, A., Geoghegon, K. F., Holmquist, B., Mortinelli, R. A., & Vallee, B. L. (1984) *Proc. Natl. Acad. Sci. U.S.A. 81*, 5041.
Auld, D. S., & Vallee, B. L. (1987) in *Hydrolytic Enzyme* (Newberger, A., & Brocklehurst, K., Eds.) pp 201–255, Elsevier, New York.
Auld, D. S., Larson, K., and Vallee, B. L. (1986) in *Zinc Enzyme* (Bertini, I., Luchinat, C., Maret, W., and Zeppezauer, M., Eds.) pp 131–154, Birkhauser, Boston.
Auld, D. S., Bertini, I., Donaire, A., Messori, L., and Moratal, J. M. (1992) *Biochemistry 31*, 3840.
Bazzone, T. J., Sokolovsky, M., Cueni, L. B., & Vallee, B. L. (1979) *Biochemistry 18*, 4362.
Bouldin, C. E. (1984) Ph.D. Thesis, University of Washington.
Bouldin, C. E., Bunker, G., McKeown, D. A., Formman, R. A., and Ritter, J. J. (1988) *Phys. Rev. B 38*, 10816.
Bunker, G. (1983) *Nucl. Inst. Mech. 207*, 437.
Bunker, G., Stern, E. A., Blankenship, R. E., & Parson, W. W. (1982) *Biophys. J. 37*, 539.
Christianson, D. W. & Lipscomb, W. N. (1989) *Acc. Chem. Res. 22*, 62.
Cox, D. J., Bovard, F. C., Bargetzi, J.-P., Walsh, K. A., & Neurath, H. (1964) *Biochemistry 3*, 44.
Cramer, S. P. (1988) in X-ray Absorption: Principle, Application, Techniques of EXAFS, SEXAFS, and XANES, (Koningsberger, D. C., & Prins, R., Eds.) p 257, John Wiley and Sons.
Crozier, E. D., Rehr, J. J., & Ingalls, R. R. (1988) in X-ray Absorption: Principle, Application, Techniques of EXAFS, SEXAFS, and XANES, (Koningsberger, D. C., & Prins, R., Eds.) p 373, John Wiley and Sons.
Gardell, S. J., Craig, C. S., Hilvert, D., Urdea, M. S., & Rutter, W. J. (1985) *Nature 317*, 551.
Hilvert, D., Gardell, S. J., Rutter, W. J., & Kaiser, E. T. (1986) *J. Am. Chem. Soc. 108*, 5298.
Horrocks, Jr., W. D., Ishley, J. N., Holmquist, B., & Thompson, J. S. (1980) *J. Inorg. Biochem. 12*, 131.
Kaiser, E. T., & Kaiser, B. L. (1972) *Acc. Chem. Res. 5*, 219.
Lange, (1956) in *Handbook of Chemistry*.
Latt, S. A., & Vallee, B. L. (1971) *Biochemistry 10*, 4263.
Lee, P. A., Citrin, P. H., Eisenberger, P., & Kincaid, B. M. (1981) *Rev. Mod. Phys. 53*, 769.
Lipscomb, W. N. (1974) *Tetrahedron 30*, 1725.
Mustre de Leon, J., Rehr, J. J., Zabinsky, S. I. & Albers, R. C. (1991) *Phys. Rev. B 44*, 4146.
Mock, W. L., & Tsay, J. T. (1988) *J. Biol. Chem. 263*, 8635.
Rees, D. C., Lewis, M., & Lipscomb, W. N. (1983) *J. Mol. Biol. 168*, 367.
Sevillano, E., Meuth, H., & Rehr, J. J. (1979) *Phys. Rev. B 20*, 4908.
Shoham, G., Rees, D. C. and Lipscomb, W. N. (1984) *Proc. Natl. Acad. Sci. U.S.A. 81*, 7767.
Spratt, T. E., Sugimoto, T., & Kaiser, E. T. (1983) *J. Am. Chem. Soc. 105*, 3679.
Stern, E. A. (1974) *Phys. Rev. B 10*, 3027.
Stern, E. A., & Heald, S. M. (1983) in *Handbook on Synchrotron Radiation*, (Koch, E. E., Ed.) pp 955–1014, Vol. 1.
Stern, E. A., Ma, Y., Hansk-Petitpierre, O., & Bouldin, C. E. (1992) *Phys. Rev. B 46*, 687.
Vallee, B. L., Riordan, J. F., & Coleman, J. E. (1963) *Proc. Natl. Acad. Sci. U.S.A. 49*, 109.
Vallee, B. L., Galdes, A., Auld, D. S., and Riordan, J. F. (1983) in *Zinc Enzymes* (Spiro, T. G., Ed.) Chapter 2, John-Wiley & Sons.
Zhang, K., Stern, E. A., Ellis, F., Sanders-Loehr, J., & Shiemke, A. K. (1988) *Biochemistry 27*, 7470.
Zhang, K., Chance, B., Auld, D. S., Larsen, K. S., & Vallee, B. L. (1992) *Biochemistry 31*, 1159.
Zhang, K., Rosenbaum, G., & Bunker, G. (1993) *Jpn. J. Appl. Phys., Part 2, 32*, 147 (Supplement).